

# GNSS GROUP DELAY VARIATIONS - POTENTIAL FOR IMPROVING GNSS BASED TIME AND FREQUENCY TRANSFER?

Tobias Kersten and Steffen Schön

Institut für Erdmessung (IfE)

Leibniz Universität Hannover

Schneiderberg 50, D-30167 Hannover, Germany

Phone: +49 511 762 5711, Fax: +49 511 762 4006

Email: {kersten | schoen}@ife.uni-hannover.de

## Abstract

*For time and frequency transfer as well as navigation applications, like, e.g., precise guided landing approaches, GNSS code observables are widely used. In addition to the well known error budget, code observables seem to be affected by Group Delay Variations (GDV), induced by the radiation pattern of the receiving antenna. The performance of the acquisition depends on the antenna and receiver ensemble. GDV degrade the precision of code observables and induce errors in timing and frequency applications.*

*In this contribution we analyzed the GDV for different antennas and receivers to quantify the net effect on the code observables and time and frequency transfer applications. The paper is divided into two parts:*

*GDV were estimated using the Hannover Concept of absolute antenna calibration with the current GNSS satellite signals in space. The GDV are parameterized using orthogonal base functions for L1(P) and L2(P) to describe variations in elevation and azimuth. Variations in elevation show magnitudes of 0.5 - 0.6 ns for the range of 90 to 30 degree and up to 1 - 2 ns at lower elevations. Azimuthal variations show smaller magnitudes, no larger than 0.6 ns for the tested sets of different GNSS antenna. The quality of the estimation process is about 0.15 ns.*

*Finally the impact on the time transfer links is investigated. A simulated time and frequency scenario with global coverage the impact and the noise contribution of the GDV are analyzed for long and short baselines equipped with different antennas. It is shown that the overall induced noise can be assigned as a white noise process with lower magnitude with respect to the existing P3 noise.*

## INTRODUCTION

Global Navigation Satellite Systems (GNSS) are not only used for navigation and positioning but are also widely adopted by timing laboratories for international time and frequency transfer as well as for clock comparisons. In parallel to the Two Way Satellite Time and Frequency Transfer (TWSTFT), three GNSS based techniques are in use: (1) GPS Common View (CV), (2) All-In-View and recently (3) Precise Point Positioning (PPP), [1], [2], [3].

Using the GPS precise P code has two advantages. First, the noise level of the P code is considerably smaller than that one of the clear access (C/A) code. Second, the first order ionospheric path delays can be

eliminated forming the ionosphere free linear combination P3, since the P code is modulated on both frequencies as signal L1 P(Y) and L2 P(Y). However, the P code may show large variations at low elevations [4] and furthermore the P code is modulated with the encrypted Y code. Therefore efforts have been made by manufacturers to develop different strategies for tracking this signal.

Since the performance of the receiver - antenna combination is important for time and frequency transfers, different error sources have to be compensated, like, e.g., hardware delays in the cable and receiver as well as the temperature sensitivity of the equipment. In this paper we will discuss the impact of the so-called Group Delay Variations (GDV), i.e. delays that are dependent on the receiver antenna and the azimuth and elevation of the incoming signal. In literature, GDV have been addressed for different applications.

It is currently discussed that GDV degrade the positioning accuracy. Examples are GNSS based landing applications [5] or satellite orbit determination. But also time and frequency transfer methods can be affected, especially when combining the 2 orders of magnitude more precise carrier phase observables with code observables [6], [7], [8]. First experiments using the Absolute Antenna Calibration unit were discussed with respect to the elevation dependent variations of the code Group Delays in [9] for several antennas and receivers. Within these studies GDV for geodetic GNSS antenna with magnitudes on order of 1 m (3.3 ns) were obtained with an accuracy of about 5 cm (0.17 ns).

The paper is organized as follows: In the first section a small experiment is discussed, that aims to visualize GDV on a short baseline in a common clock setup. Next we propose a methodology to determine the variations and discuss the obtained GDV magnitudes for several geodetic antennas. In the last section we analyze the possible impact of the GDV on time and frequency transfer for European and transatlantic links using different simulation scenarios.

## ANALYSIS OF GDV IN THE OBSERVATION DOMAIN

In order to get a first impression of the range of possible GDV in GNSS code observations, a test setup was installed at the laboratory network at the rooftop of the Institut für Erdmessung (IfE), University Hannover. On a small baseline (approx. 7 m), seven hours of observations were taken in a static scenario with 1 Hz sampling frequency, cf. Figure 1. To avoid individual receiver clock errors introduced by the Javad TRE-G3T receivers, an external Rubidium Frequency Standard FS725 from Stanford Instruments was used as common clock. During the investigations constant thermal conditions are given for a  $\mu$ Blox antenna ANN-MS\_GP and a Javad Dual Depth Choke Ring JPS\_REGANT\_DD\_E antenna mounted on pillar msd7 and msd8, respectively, cf. Figure 2. Also other combinations of geodetic antennae on a short baseline were analyzed. Therefore we used a Leica AR25 Rev. 3 antenna on MSD8, while on MSD7 different geodetic antennas were installed.

For accessing GDV on observation level, we apply an approach similar to these using carrier phase observations as shown in [10] as well as [11]. Starting with the undifferenced code observation  $P_A^j$  in meters from a satellite  $j$  to a station  $A$  reads:

$$P_A^j = \rho_A^j + c(\delta t_A - \delta t^j) + T_A^j + I_A^j + d_A - d^j + REL_A^j + MP_A^j + GDV(\alpha, e) + \epsilon_A^j \quad (1)$$

with the geometric distance  $\rho_A^j$ , the receiver  $c\delta_A$  and satellite  $c\delta^j$  clock error in meters, the signal delay in the receiver  $d_A$  and at the satellite  $d^j$ , the relativistic effect  $REL_A^j$ , the multipath error  $MP_A^j$  and code noise  $\epsilon_A^j$ , as well as the primary error sources: the tropospheric path delay  $T_A^j$  and the ionospheric path delay  $I_A^j$ ,

[12]. We introduce the Group Delay Variation  $GDV(\alpha, e)$  to the code observables as a function of elevation and azimuth of the incidence ray.

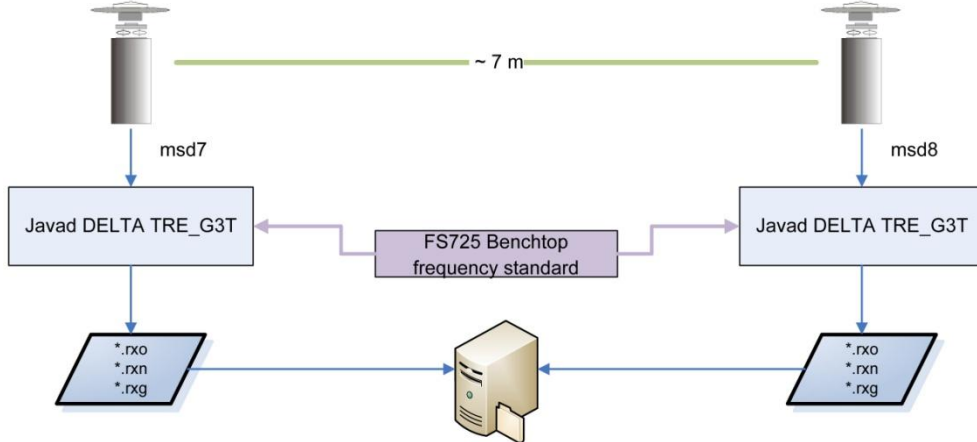
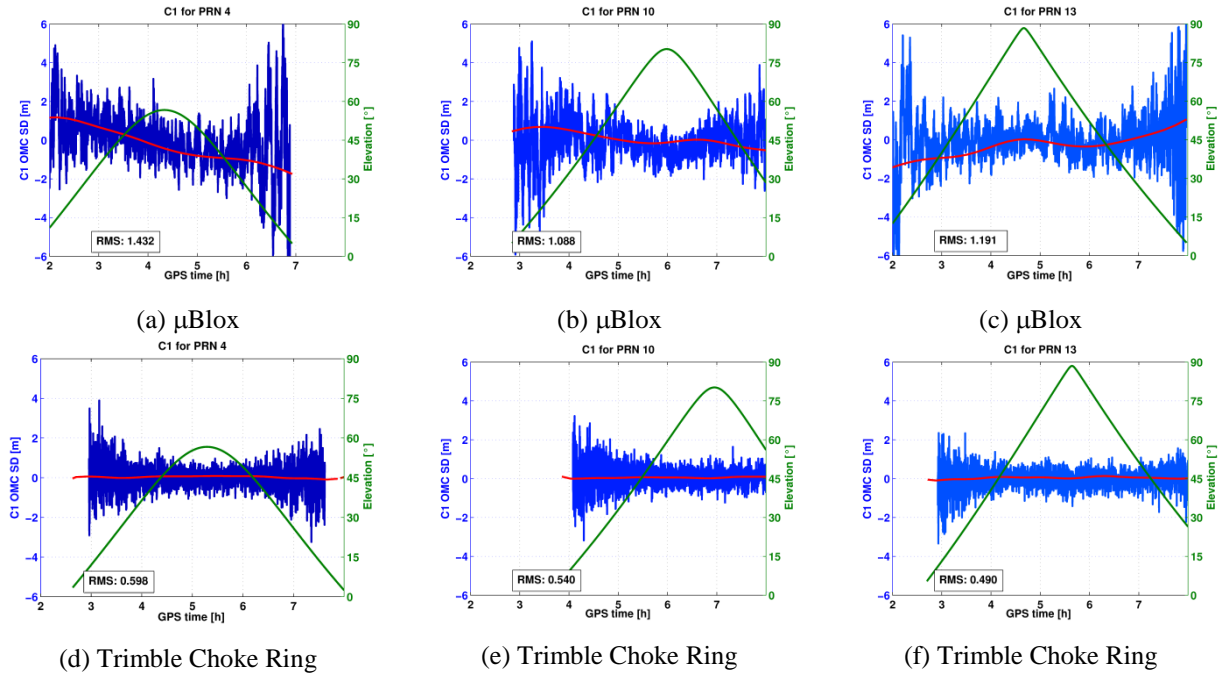


Figure 1. Sketch of the installed setup of a short baseline with similar receivers steered by an external FS725 Rubidium Frequency Standard.



For the elimination of distance dependent effects as well as effects induced by the satellite clock, inter-station single differences  $SD_{AB}^j = P_A^j - P_B^j$  are formed:

$$SD_{AB}^j(t_i) = GDV_{AB}^j(\alpha, e, t_i) + MP_{AB}^j + c\Delta\delta_{AB}(t_i) + \epsilon_{AB}^j(t_i) \quad (2)$$

with the differential Group Delay Variation  $GDV_{AB}^j(\alpha, e, t_i)$ , the effect of multipath at both stations  $MP_{AB}^j(t_i)$  the differential receiver clock error  $c\delta t_{AB}(t_i)$  in meter, as well as the code noise  $\epsilon_{AB}^j(t_i)$  with a magnitude of  $\sqrt{2} \cdot \epsilon_A^j(t_i)$ .

Since a Stanford Rubidium FS725 was used as common clock, the individual receiver clock errors evaluate identically over time. Thus the differential receiver clock error is constant. Its amount equals the initial clock offset between both receivers.

Exemplary Observed Minus Computed (OMC) values of SD for some GPS satellites are shown for a low cost and high sensitive  $\mu$ Blox patch antenna in Figure 2(a)-(c). Long-periodic systematic variations with magnitudes of up to 3 ns and individual for every satellite can be noticed. These systematics can be referred to the differences of the GDV of both antennae that change with the incident (azimuth and elevation) angle of every satellite in the antennae body frame. In Figure 2(a)-(c), an elevation dependent pattern is visible. However since variations differ for satellites with a different constellation, one can also assume variations in azimuth.

The same experimental setup was used with other geodetic antennas which show only small variations within magnitudes of lower than 0.5 ns. One example of a baseline equipped with typical GNSS choke ring antennae is presented in the Figure 2(d)-(f) where possible GDV are definitely below 1 ns.

## CONCEPT OF GDV DETERMINATION

With the Hannover Concept of Absolute Antenna Calibration an excellent experiment and calibration facility exists. Since 2000, Phase Center Variations (PCV) for GPS and GLONASS carrier phases on frequencies L1/L2 are successfully and routinely determined as described in detail in [13], [14], [10]. We adopted this technique and expand the algorithms in our IfE software package to use this approach for obtaining GDV with the actual available modulated GNSS signals in the field. The facility as well as the principle of this approach is shown in Figure 3.

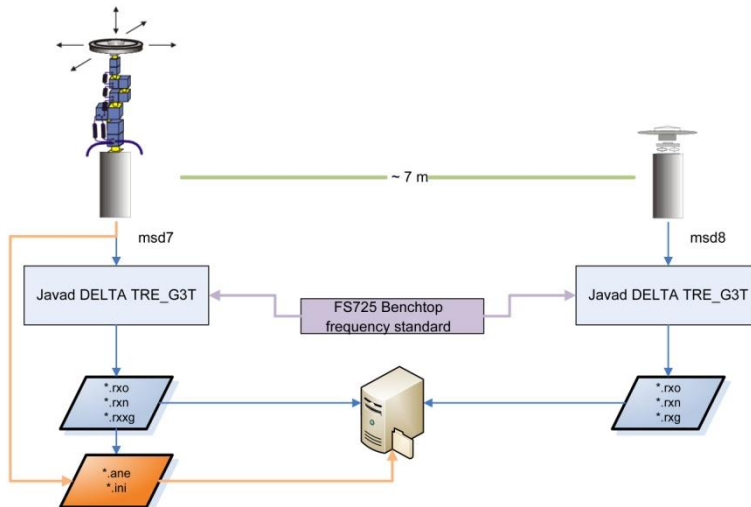


Figure 3. Calibration Facility of the Hannover Concept for Absolute Antenna Calibration at the Institut für Erdmessung, University of Hannover.

## OBSERVATION MODEL OF GROUP DELAY VARIATIONS (GDV)

Using the advantage of eliminating several errors sources by applying inter-station single differences like in equation (2) would largely reduce the GDV as well. However, if the orientation of the antenna under test is changed in very precise and predictable steps between subsequent epochs, we eliminate the impact of the reference antenna and access the GDV of the test-antenna at epoch  $t_i$  like

$$\Delta SD_{AB}^j(t_i) = SD_{AB}^j(t_{i-1}) - SD_{AB}^j(t_i) \quad (3)$$

which yields to the observation equation for the GDV within the estimation process

$$\Delta SD_{AB}^j(t_i) = \Delta GDV_A^j(t_{i-1}, t_i) + \Delta MP_{AB}(t_{i-1}, t_i) \quad (4)$$

Due to the maximum offset of 5 seconds between subsequent epochs the multipath term at station  $B$  is eliminated and largely reduced for the antenna under test on the robot arm. Since both receivers are connected to a Stanford Rubidium FS725, the differential receiver clock error is assumed to vanish - the impact is at least below the noise level of the code observation of  $1 - 2 \cdot 10^{-9} \cdot \tau^{-1}$ . The specification of the FS725 provides a stability of less than  $\sigma_y = 2 \cdot 10^{-11} \cdot \tau^{-0.5}$  that corresponds to  $\sigma_y = 1.5 \cdot 10^{-11}$  for 5 seconds. This is much smaller than the white code noise  $\sigma_y = 1.8 \cdot 10^{-10} \cdot \tau^{-1}$ , so that the code noise is dominant.

The robot arm itself was calibrated with a LEICA laser tracker LTD 640 at the Geodetic Institute of Hannover (GIH). It was proven that the positioning is accurate at the 0.25mm level [15].

## MATHEMATICAL MODEL OF GROUP DELAY VARIATIONS (GDV)

In analogy to the approach of determining PCV, we use continuous expansions on a sphere for suitably modelling GDV as variations with orthogonal base - functions. For subsequent epochs the observation equation for the parameter estimation reads

$$f(\alpha, e) = GDV(\alpha_0, e_0, t_{i-1}) - GDV(\alpha_0 + \Delta\alpha, e_0 + \Delta e, t_i) \quad (5)$$

which can be expanded into a series of fully normalized harmonics  $\bar{R}_{nm}$  and  $\bar{S}_{nm}$  like

$$GDV(\alpha, e) = \sum_{n=0}^{n_{max}} \sum_{m=0}^{m_{max}} \{ A_{nm} \bar{R}_{nm}(\alpha, e) + B_{nm} \bar{S}_{nm}(\alpha, e) \}$$

with:  $A_{nm}, B_{nm} :=$  unknown coefficients (6)

$$\begin{cases} \bar{R}_{nm}(\alpha, e) \\ \bar{S}_{nm}(\alpha, e) \end{cases} = \begin{cases} \cos(m\alpha) \\ \sin(m\alpha) \end{cases} N_{nm} P_{nm}(\sin e)$$

and with the degree  $n$  and order  $m$  of the spherical expansion, the elevation angle  $e$  and azimuth angle  $\alpha$  of a satellite in the topocentric antenna system, the normalization factor  $N_{nm}$  and the associated Legendre functions  $P_{nm} \sin(e)$ , cf. [16].

The estimation procedure is implemented in the software package developed at the Institut für Erdmessung. Details as well as results of a co-variance analysis of the estimable parameter are described

in [11]. The spherical harmonic coefficients are obtained, to calculate the corrections from a synthesis by the spherical harmonics.

## DISCUSSION OF GROUP DELAY VARIATIONS (GDV)

Applying the above mentioned methodology we estimate parameter sets for different non-geodetic and geodetic antennas, which have different properties. In Table 1, numerical values for the estimated GDV are listed for the antenna used within this study. The table reads as follows: the column AZI gives the minimum and maximum GDV value of azimuthal variations down to an elevation angle of 10°. The column NOAZI indicates also the minimum and maximum values but assuming no azimuthal variations. Comparing the columns in Table 1, differences between the antennae are obvious. Additionally, note that differences between the GDV of C/A code and P code occur, especially for the Ashtech Marine and the µBlox antennas. Azimuthal variations for some antennas are large and significant, so that numerical values of up to 6 ns for C/A and up to 2.6 ns for P code at an elevation angle of 10° are visible. In the same way it has to be mentioned that variations in elevation are smaller in magnitude than for azimuth within the range of 90° down to 30° of elevation on P code. This is an indication that (1) Group Delays exist at receiver antennas and (2) they vary with the azimuth incidence angle and (3) different antennas show different behavior. Referring to [9], similar results for GDV determination are discussed.

Table 1. Numerical maximum and minimum values of estimated GDV.

Antenna	Dome	GPS GDV					
		C/A		P1		P2	
		AZI [ns]	NOAZI [ns]	AZI [ns]	NOAZI [ns]	AZI [ns]	NOAZI [ns]
µBlox	NONE	6.0	0.6				
Ashtech Marine L1L2	NONE	4.0	0.5	2.3	1.3	2.6	1.3
Leica AR 25	LEIT	-	-	0.2	1.0	0.3	1.1
Trimble Zephyr Geodetic I	NONE	-	-	2.6	1.2	2.5	1.3
Trimble Choke Ring	NONE	-	-	1.5	1.1	1.7	1.3

Furthermore some similarities of the GDV pattern for the antennas we used in this study exist with respect to their corresponding Phase Center Variation (PCV) pattern (which can be determined for the carrier phase frequencies) especially for antennas which showing large azimuthal variation within their PCV.

Retrieved GDV in dimension of nanoseconds are depicted for some antennas in Figure 4. For the calibrated µBlox antenna azimuthal variations on C/A have magnitudes of up to 2-3 ns for elevation angles between 90°-30°. These azimuthal variations produce the overall effect, which can be seen in Figure 2. For the Ashtech Marine Antenna we present in Figure 5(b) only the GDV on C/A although also GDV on P1 and P2 were estimated. GDV for P1 and P2 show a similar behavior with a reduced magnitude of 1.2 - 1.5 ns in comparison to the C/A code.

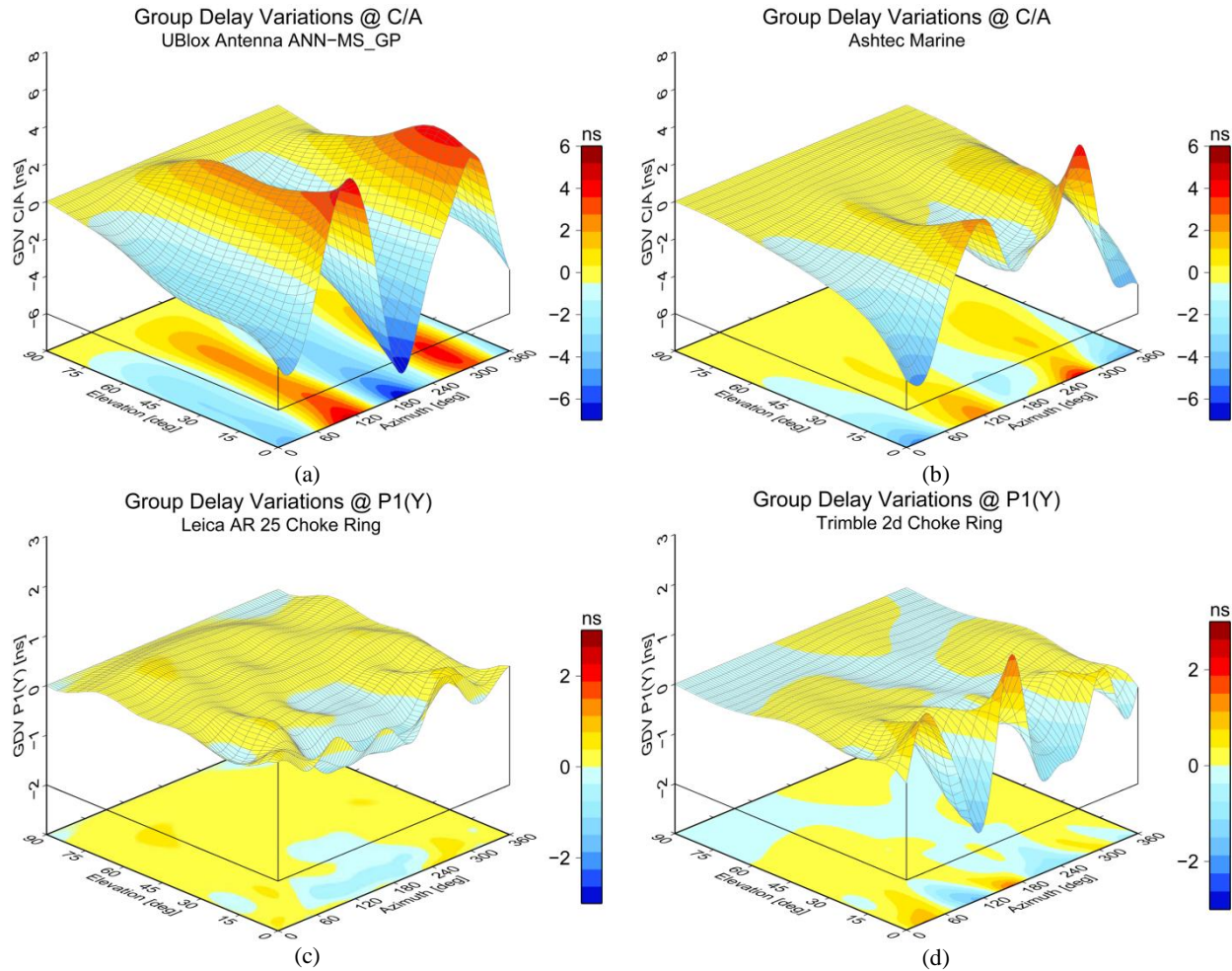


Figure 4. Determined GDV for several low cost and high performance antennas.

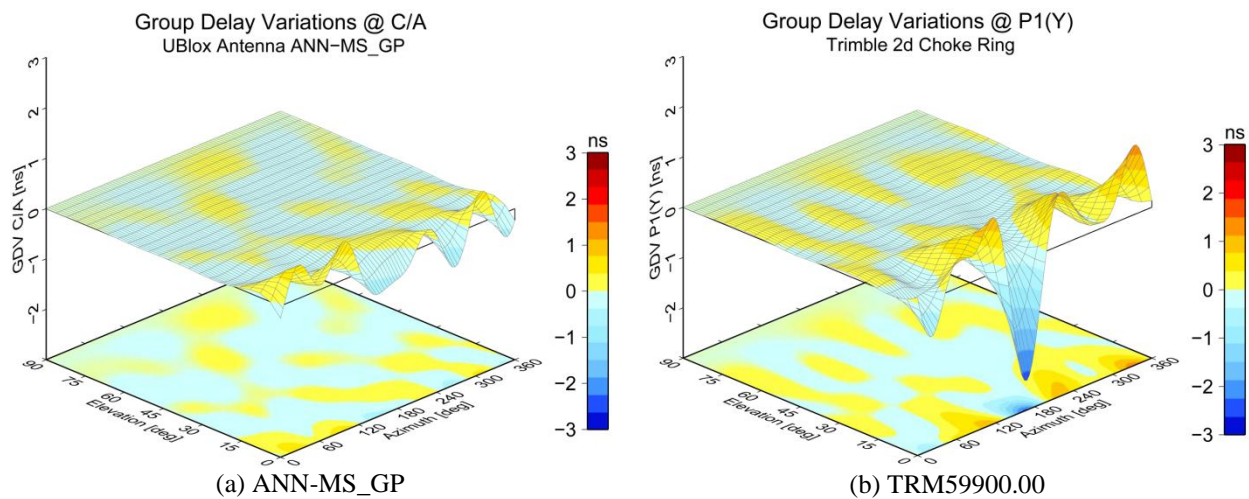


Figure 5. Determined GDV for one low cost and one high performance antenna.

In contrast, geodetic antennas do not show significant differences between elevation and azimuthal variations, although they exist with a magnitude of up to 1.7 ns for a typical choke ring antenna and 2.6 ns for a Trimble Zephyr Geodetic I TRM41249.00. Within this study GDV of the Leica LEIAR25 Antenna shows very small variations in azimuth. The pattern is dominated by variation in elevation; cf. Figure 4(c).

## PLAUSIBILITY CHECKS

Since the code noise is large compared to the pattern, the following plausibility checks for the determined GDV were carried out. To this end the estimated GDV were applied to the observations which were used for the calibration. For every epoch and line of sight to a satellite, GDV were calculated. Afterwards these GDV corrections are introduced as  $GDV(\alpha, e)$  to the observation equation from equation (6). Since the previously estimated GDV values are introduced and a second estimation of spherical harmonics is carried out, all resulting variations are related to the noise of the estimation process.

Results are depicted in Figure 5 for C/A code estimated GDV at the  $\mu$ Blox antenna and P code estimated GDV for Trimble 2d Choke Ring TRM59900.00 antenna. Only small variations of 0.10 - 0.25 ns at elevations between  $90^\circ$  down to  $15^\circ$  are noticeable. The estimation process itself has an uncertainty of about 0.15 ns (4.5 cm), which is less than one-tenth of the code noise of the input data. Thus GDV seems to be significant and estimable with the Hannover Concept of Absolute Antenna Calibration.

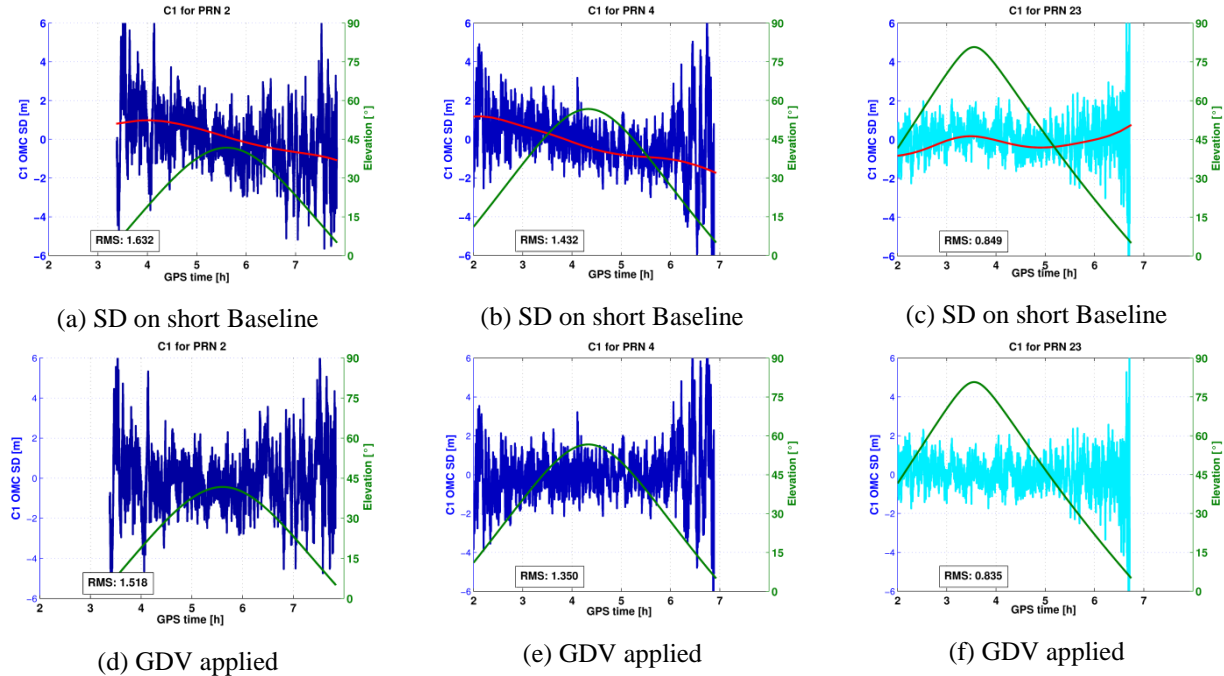


Figure 6. Inter-station single differences (SD) on a short baseline equipped with low cost and high performance antennas in common clock mode. In the subplots (a) - (c) elevation and azimuth dependent effects are obviously existent. These effects can be reduced by applying determined Group Delay Variations (GDV).

A second verification use the static setup on a short baseline as depicted in Figure 1. To be really certain that systematic variations in Figure 2(a)-(c) are dominated by GDV, we evaluate the corrections per epoch and line-of-sight to apply them to the OMC of the C/A code measured on this baseline. Although there were no GDV applied for the Javad Dual Depth JPS\_REGANT\_DD\_E antenna on pillar MSD8,

systematic errors could be largely reduced for C/A as depicted in Figure 6 since the GDV of the  $\mu$ Blox ANN-MS\_GP antenna on pillar MSD7 dominates the impact with magnitudes of up to 3 ns.

Further evaluations were done using the same setup with a Trimble Zephyr I TRM41249.00 and a Leica AR25 LEIAR25 antenna mounted on pillars MSD7 and MD8, respectively. These evaluations were carried out with 100-second smoothed P1 code and a sampling frequency of 5 Hz. It shows that applying the GDV for both antenna on a short baseline improves the code observation in the mean elevations about 0.6 - 0.8 ns. This gets clear since the difference between the GDV of both antennas on a short baseline vary significantly from each other for one specific line-of-sight of a satellite. In other words: since the radiation patterns of both antennas vary significantly from each other, the observations from one satellite to these antennas vary in the range of the difference plus additional noise.

## APPLICATION TO TIME TRANSFER

Additional to the discussion of [9], we can also show that (1) GDV exist for receiver antennas, (2) they can be determined using the Hannover Concept of Absolute Antenna Calibration with uncertainties of approximate by 0.15 ns and (3) applying GDV correction on a short baseline can largely reduce the systematic errors.

To analyze the impact of GDV on time and frequency transfer and clock comparisons we have to face the questions (1) which noise contribution can be expected from the GDV on different continental and inter-continental links and (2) can this GDV correction improve the uncertainties for code based ionosphere free P3 time and frequency applications?

### SIMULATION STRATEGY

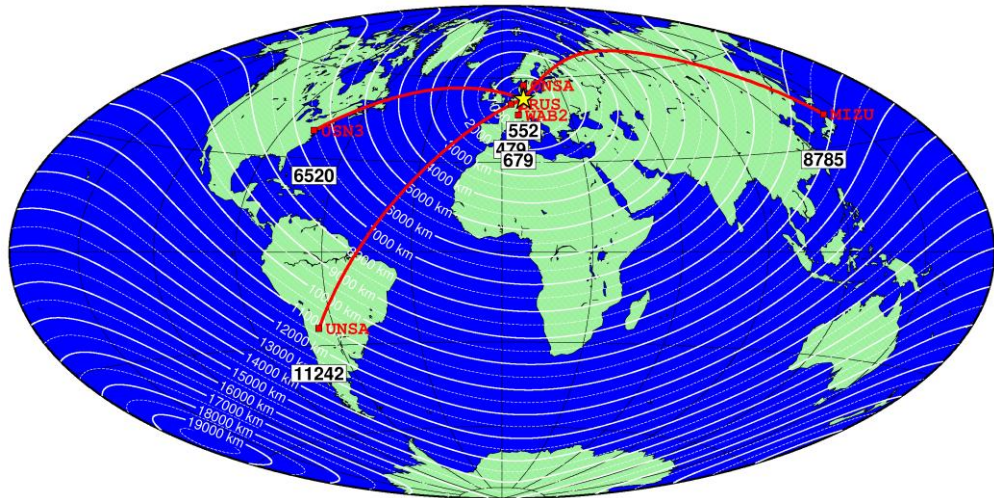


Figure 7. Links between ITRF2008 and IGS stations used within the simulation study.

The GDV are introduced in a simulation. We processed several times 14 days in daily batches with a sampling rate of 15 seconds for 7 stations, each equipped with four different antennas: (1) Ashtech Marine ASH700700.B, (2) Leica AR25 LEIAR25, (3) Trimble Zephyr I TRM41249.00, and (4) Trimble 2d choke ring TRM59900.00 antenna, to evaluate the possible impact of different antenna combinations

on different links. The stations used within this study and shown in Figure 7 are ITRF and IGS stations. Besides inner-European links, stations outside Europe were used to vary the GPS satellite geometry.

The clock is estimated using the ionosphere free linear combination on P3 which reads

$$P_3 = \left( \frac{f_1^2}{f_1^2 - f_2^2} \right) P_1 - \left( \frac{f_2^2}{f_1^2 - f_2^2} \right) P_2 \quad (7)$$

with  $f_1$  and  $f_2$  being the corresponding carrier phase frequencies. From experiments done at the laboratory network at the IfE rooftop with different antennas and receivers, a P1 code noise of  $\sigma_P \approx 0.5$  m at 1 Hz and mean elevation was obtained. This yields to a P3 code noise of  $\sigma_{P_3} \approx 1.5$  m (5 ns) at 1 Hz sampling frequency.

Precise orbits from the IGS [17] as well as the IfE software package were used for the simulations. The applied time transfer methodology equals the All-In-View technique since all satellites visible above an elevation of  $5^\circ$  are considered. The advantage of using All-In-View with respect to Common-View techniques is discussed in detail in [18].

## STABILITY ANALYSIS

For every station, solutions with four antennae are obtained, each set with 80640 epochs (at 15 seconds sampling rate), of clock bias estimates. Different links lengths were selected and exemplary results are depicted in Figure 8(a). The induced time transfer error for the link PTBB - BRUS with the same antenna is +0.05 ns whereas for an inter-continental link PTBB - UNS3 equipped with the same antenna this rises to -0.08 ns. However, the largest impact could be obtained for a inter-continental link PTBB - UNS3 and different antennae (ASH700700.B vs. TRM59900.00) with a time transfer error of -0.35 ns. Typical pattern is induced by the changing satellite geometry which is repeated with the well known sidereal repetition time of 24 h - (3 min 56 sec).

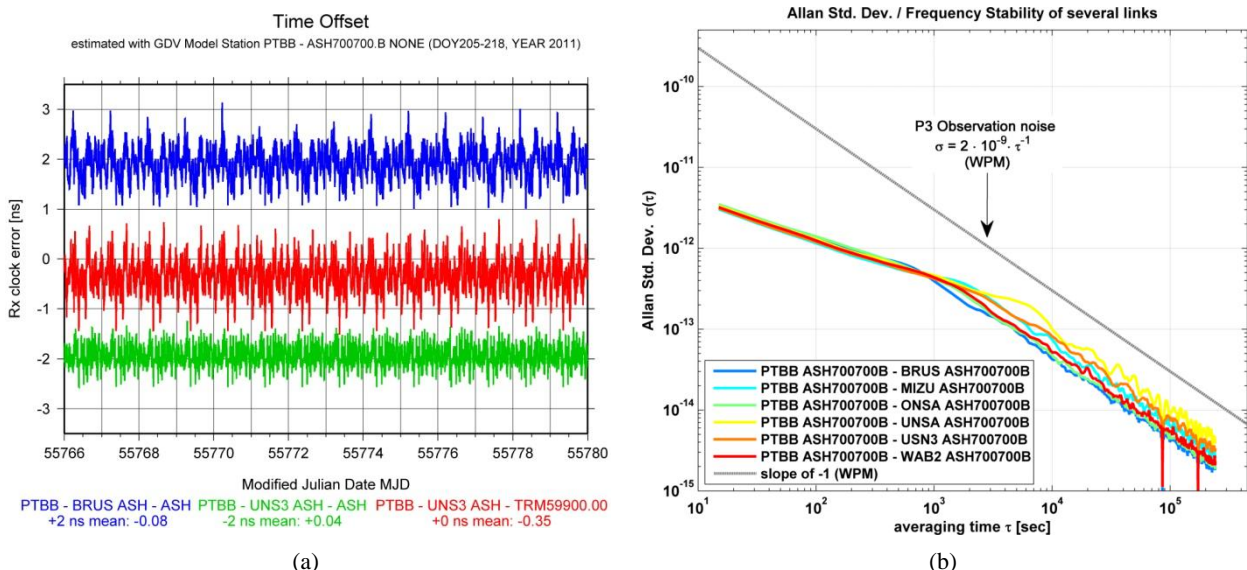


Figure 8. Simulated time series of estimated receiver clock error for three exemplarily links from PTBB are shown in (a). Plot of the Allan Deviation for different links are shown in (b), assuming that every station is equipped with the same antenna.

In Figure 8(b) the Allan Deviation [19], [20] of several links, for simulation purposes equipped with same antenna type, are shown. It is obvious that the Allan Deviation starts with a flicker white noise frequency modulation (WFM) with a slope of  $\tau^{-0.5}$  until  $\tau = 1000$  sec ( 20 minutes). Then the noise of the links turns to a white noise phase modulation (WPM) characteristic with a slope of  $\tau^{-1}$ . For comparison, the Allan Deviation of a P3 white phase noise is added in Figure 8(b). A stability of  $\sigma_y = 3 \cdot 10^{-9}$  at  $\tau = 1$  is assumed, which is quite reasonable for the observation noise of P3 links shown in [21] as well as [4].

For a short link PTBB-BRUS and for the same antenna, the plot of the Allan Deviation shows a stability of  $\sigma_y = 4 \cdot 10^{-13}$  at  $\tau = 1000$  seconds, quite similar for an inter-continental link PTBB - UNS3.

But significant differences occur due to the different GPS satellite geometry. This is obvious since the Aschtech Marine antenna has a pronounced GDV pattern, which is similar but not equal to the GDV pattern on C/A, cf. Figure 4(b). These variations accentuate for increasing length of the time link. The behavior of the Allan Deviation is very similar for all of our tested antennas, especially referring to the characteristic cut-off frequency. The transition between the different noise processes always occurs around  $\tau = 10^3$  seconds. For all antenna combinations the impact is well below the P3 observation noise of the links. With the upcoming new GNSS signals, GDV will become more critical. However, since the impact of the GDV on the estimated clock bias is smaller than the expectable noise using P3 and IGS orbits, this impact is insignificant since only P3 is considered.

## STABILITY ANALYSIS WITH GGTTS

To provide comparable values within the time and frequency transfer, the simulated time series were analyzed using the GPS time transfer standardization. The Comité Consultatif pour la Définition de la Seconde (CCDS) formed the Group on GPS Time Transfer Standards (GGTTS) to draw up standards for the use of GPS time receivers for time and frequency applications and international clock comparisons. The established GGTTS format is a unique standard for GPS time receiver software and applications. One track of the GGTTS formats consists of 780 seconds (13 minutes) length. The reasons for the 13 minutes are (1) usually a receiver required 2 minutes to lock on one satellite, (2) approximately 10 minutes are necessary to transmit the full content of the navigation message and (3) one minute is used for data processing and preparation of a new track [22].

Simulated time series for the several antennae and links are transformed into the GGTTS format and depicted for the time link PTBB -BRUS, PTBB - MIZU, PTBB - UNS3 and PTBB -WAB2 in Figure 9(a) for the Ashtech Marine ASH700700.B and in Figure 9(b) for a Trimble Choke Ring TRM59900.00 antenna. Starting from the GGTTS Allan Deviation of the Ashtech antenna, a typical white noise phase modulation process (WPM) is obvious with a slope of  $\tau^{-1}$ . As expected, the smallest Allan Deviation is obtained for the short link PTBB -BRUS, assuming that the same antennas are in use, since the impact of GDV is largely reduced in a similar geometry. Comparing to Figure 9(b) this behavior is similar. For inter-continental links the Allan Deviation starts with a white frequency modulation (WFM) of  $\sigma_y = 2.1 \cdot 10^{-11} \cdot \tau^{-0.5}$ , cf. also Figure 8(b), followed by a white phase modulation (WPM) process with  $\sigma_y = 5 - 8 \cdot 10^{-10} \tau^{-1}$ , for  $\tau > 1000$  seconds.

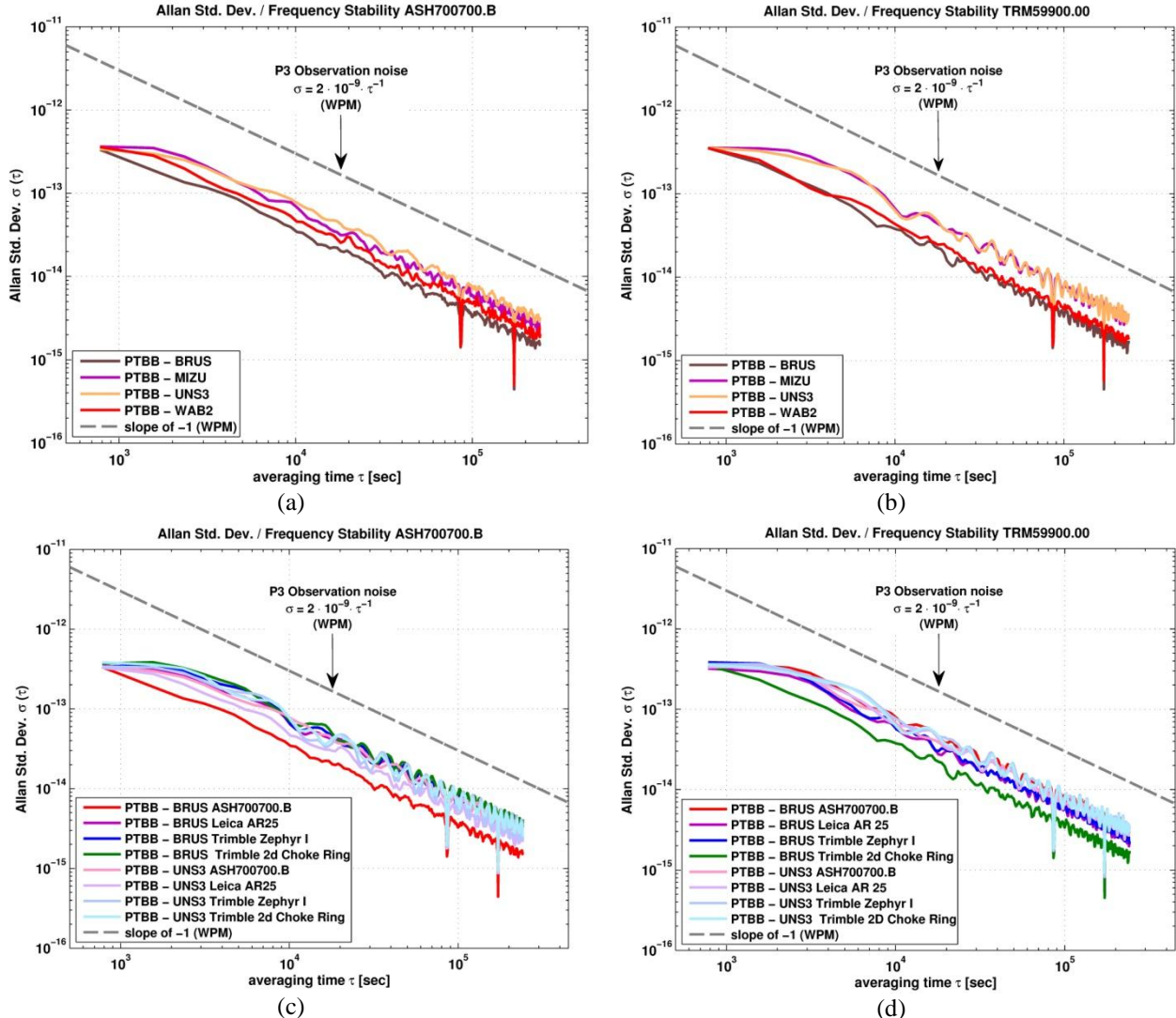


Figure 9. Allan standard deviation of simulated time series in GGTTS format for several baselines and different equipment.

For the time series of links equipped with different antennas and different behavior of the GDV pattern the situation is depicted in Figure 9(c) as well as 9(d). The best results can be achieved assuming that both stations of a short link are equipped with the same antennas. For long links this is not true. It depends on the GDV as well as of the changing satellite geometry. Within our analysis all the GDV of the antennas show a quite similar behavior. Since the P3 code noise is slightly larger than the effect introduced by the GDV, we summarize that within the GGTTS time format the GDV are not yet an issue for the stability of the link. However, the apparent noise induced by the GDV is close to the noise achievable by combining carrier phase and code observables. The phase noise of the Code plus Carrier linear combination (CPC) is reduced by a factor of about 20 with respect to the P3 code noise [7]. Also potential GDV for the Galileo E5a,b AltBOC signal could have an impact since the observation noise is largely reduced.

## CONCLUSION

In this study we have shown that a significant systematic error on code observables is induced by Group Delay Variations (GDV). They vary for elevation as well as azimuth of incidence angle and are unique for different antennas. It could also be shown that these GDV can be estimated by the Hannover Concept of Absolute Antenna Calibration. The methodology provides a precision of 0.15 ns and is implemented in the IfE software package. Furthermore, significant errors on short baselines could be reduced when applying these corrections.

Within a simulation analysis the effect of GDV equals a white noise phase/flicker modulation (WPM/FPM) with a slope of  $\tau^{-1}$  and an uncertainty of  $\sigma_y = 2 - 3 \cdot 10^{-12}$  at  $\tau = 1000$  seconds. The same behavior can be expected if applying the CCDS defined GGTTS standard format for time and frequency applications. Since the noise level of P3 is very high ( $\approx 2 \cdot 10^{-11}$  at  $\tau = 1000$ ) the impact induced by the GDV on the estimated receiver clock bias is up to now insignificant.

GDV can induce time offsets in the link up to 0.41 ns for the analyzed high end and up to 0.58 ns for a combination of high end and low cost antennae.

Further investigations are necessary facing the code and carrier phase combination methods, which will improve the stability and precision of time transfer applications. Here GDV can become an issue. Even though new generations of code signals with a very low code noise will be fully available within the next decade and improve time and frequency transfer as well. They will decrease the code noise level significantly and this will open the door for the GDV, so that they have to be modeled accurately for the use in precise applications.

Further investigations will be also concentrated on an improved model regarding the tracking loops in the receiver, since they are an important parameter within the code observable. It could be shown, that the GDV for several antenna have magnitudes of more than one full carrier wavelength. This would possibly contribute to improve the ambiguity fixing, especially in Precise Point Positioning (PPP) applications, since they are also frequently used in precise time and frequency transfer techniques.

## DISCLAIMER

Although the authors dispense with endorsement of any of the products used in this study, commercial products are named for scientific transparency. Please note that a different receiver / antenna unit of the same manufacturer and type may show a different behavior.

## ACKNOWLEDGMENT

The work within this project is supported by the German Aerospace Center (DLR) with the project label 50NA0903, funded by the Federal Ministry of Economics and Technology (BMWI), based on a resolution by the German Bundestag.

## REFERENCES

- [1] A. Gifford, 2000, “*One Way GPS Time Transfer 2000*,” in 32nd Annual Precise Time and Time Interval (PTTI) Meeting.
- [2] J. Levine, 2008, “*A Review of Time and Frequency Transfer Methods*,” **Metrologia**, **45**, 162–174.
- [3] M. A. Lombardi, L. M. Nelson, A. N. Novick, and V. S. Zhang, 2001, “Time and Frequency Measurements Using the Global Positioning Systems,” **Cal. Lab. Int. J. Metrology**, **3**, 26–33.
- [4] H.-M. Peng, C.-S. Liao, and J.-K. Hwang, 2005, “*Performance Testing of Time Comparison Using GPS-smoothed P3 Code and IGS Ephemeris*,” **IEEE Transactions on Instrumentation and Measurement**, **54**(2), 825–828.
- [5] T. Murphy, P. Geren, and T. Pankaskie, 2007, “*GPS Antenna Group Delay Variation Induced Errors in a GNSS Based Precision Approach and Landing Systems*,” in Proc. ION GNSS 20th International Technical Meeting of the Satellite Division, 25–28 September 2007, Fort Worth, Texas, USA.
- [6] G. Cerretto, A. Perucca, P. Pavella, A. Mozo, R. Píriz, and M. Romay, 2010, “*Network Time and Frequency Transfer With GNSS Receivers Located in Time Laboratories*,” **IEEE Transactions on Ultrasonics, Ferroelectronics and Frequency Control**, **57**(6), 1276–1284.
- [7] P. Defraigne, 2011, “*GNSS Time and Frequency Transfer: state of the art and possible evolution*,” in Workshop on Development of Advanced TFT Techniques, Bureau Internationale des Poids et Measurements (BIPM), 28 June 2011.
- [8] J. Ray and K. Senior, 2003, “*IGS/BIPM pilot project: GPS carrier phase for time/frequency transfer and timescale formation*,” **Metrologia**, **40**, 270–288.
- [9] G. Wübbena, M. Schmitz, and M. Propp, 2008, “*Antenna Group Delay Calibration with the Geo++ Robot - extensions to code observable*,” in IGS Analysis Workshop, Poster, 2-6 June 2008, Miami Beach, Florida, USA.
- [10] G. Wübbena, M. Schmitz, F. Menge, V. Böder, and G. Seeber, 2000, “*Automated Absolute Field Calibration of GPS Antennas in Real-Time*,” in ION GPS 2000, 19-22 September 2000, Salt Lake City, Utah, USA.
- [11] T. Kersten and S. Schön, 2010, “*Towards Modeling Phase Center Variations for Multi-Frequency and Multi-GNSS*,” in 5<sup>th</sup> ESA Workshop on Satellite Navigation Technologies and European Workshop on GNSS Signals and Signal Processing (NAVITEC), 8-10 December 2010 ESTEC, Noordwijk, The Netherlands.
- [12] B. Hofmann-Wellenhof, H. Lichtenegger, and E. Wasle, editors, 2008, **GNSS - Global Navigation Satellite Systems, GPS, GLONASS Galileo and more**, Springer, Wien - New York.
- [13] F. Menge, 2003, “*Zur Kalibrierung der Phasenzentrumsvariationen von GPS Antennen für die hochpräzise Positionsbestimmung*,” PhD thesis, Wissenschaftliche Arbeiten der Fachrichtung Vermessungswesen der Universität Hannover, Hannover, Germany.

- [14] F. Menge, G. Seeber, C. Völksen, G. Wübbena, and M. Schmitz, 1998, “Results of the absolute field calibration of GPS antenna PCV,” in Proc. Int. Tech. Meet ION GPS-98, Nashville, Tennessee, USA.
- [15] V. Meiser, 2009, “*Kalibrierung des GNSS-Antennenkalibrierroboters des Institut für Erdmessung mittels Lasertracking*,” Technical Report, Geodätisches Institut Hannover, Hannover, Germany.
- [16] E. Hobson, 1931, **The Theory of Spherical and Ellipsoidal Harmonics**. Cambridge, University Press.
- [17] J. M. Dow, R. Neilan, and C. Rizos, 2009, “*The International GNSS Service in a changing Landscape of Global Navigation Satellite Systems*,” **Journal of Geodesy**, **83**, 191–198, Springer Verlag, New York.
- [18] M. A. Weiss, G. Petit, and Z. Jiang, 2005, “*A Comparison of GPS Common-View Time Transfer to All-in-View*,” in Frequency Control Symposium and Exposition, 2005, Proceedings of the 2005 IEEE International, 29-31 August 2005.
- [19] D. W. Allan, 1966, “*Statistics of Atomic Frequency Standards*,” **Proceedings of the IEEE**, **54**(2), 221–230.
- [20] D. W. Allan, 1987, “*Time and Frequency (Time-Domain) Characterization, Estimation and Prediction of Precision Clocks and Oscillators*,” **IEEE Transactions on Ultrasonics, Ferroelectrics, and Frequency Control**, **UFFC-34**(6), 647–654.
- [21] P. Defraigne and G. Petit, 2003, “*Time transfer to TAI using geodetic receivers*,” **Metrologia**, **40**, 184–188.
- [22] D. W. Allan and C. Thomas, 1994, “*Technical Directives for Standardization of GPS Time Receiver Software to be implemented for improving the accuracy of GPS common-view time transfer*,” **Metrologia**, **31**, 69–79.

